TISSUE ENGINEERING: Part A
Volume 18, Numbers 5 and 6, 2012

DOI: 10.1089/ten.tea.2011.0195

Intervertebral Disk Tissue Engineering Using Biphasic Silk Composite Scaffolds

Sang-Hyug Park, Ph.D.,[1] Eun Seok Gil, Ph.D.,[1] Hongsik Cho, Ph.D.,[2] Biman B. Mandal, Ph.D.,[1] Lee W. Tien, M.S.,[1] Byoung-Hyun Min, M.D., Ph.D.,[3,4] and David L. Kaplan, Ph.D.[1]

Scaffolds composed of synthetic, natural, and hybrid materials have been investigated as options to restore intervertebral disk (IVD) tissue function. These systems fall short of the lamellar features of the native annulus fibrosus (AF) tissue or focus only on the nucleus pulposus (NP) tissue. However, successful regeneration of the entire IVD requires a combination approach to restore functions of both the AF and NP. To address this need, a biphasic biomaterial structure was generated by using silk protein for the AF and fibrin/hyaluronic acid (HA) gels for the NP. Two cell types, porcine AF cells and chondrocytes, were utilized. For the AF tissue, two types of scaffold morphologies, lamellar and porous, were studied with the porous system serving as a control. Toroidal scaffolds formed out of the lamellar, and porous silk materials were used to generate structures with an outer diameter of 8 mm, inner diameter of 3.5 mm, and a height of 3 mm (the interlamellar distance in the lamellar scaffold was 150–250 μm, and the average pore sizes in the porous scaffolds were 100–250 μm). The scaffolds were seeded with porcine AF cells to form AF tissue, whereas porcine chondrocytes were encapsulated in fibrin/HA hydrogels for the NP tissue and embedded in the center of the toroidal disk. Histology, biochemical assays, and gene expression indicated that the lamellar scaffolds supported AF-like tissue over 2 weeks. Porcine chondrocytes formed the NP phenotype within the hydrogel after 4 weeks of culture with the AF tissue that had been previously cultured for 2 weeks, for a total of 6 weeks of cultivation. This biphasic scaffold simulating in combination of both AF and NP tissues was effective in the formation of the total IVD *in vitro*.

Introduction

Intervertebral disk (IVD) degeneration occurs because of a variety of factors, resulting in a multitude of complications for the patient. Aging, differences in collagen distribution, vascular in-growth, mechanical loads placed on the disk, and changes in the matrix composition (larger average hydrodynamic size and higher glucosamine to galactosamine ratio) can contribute to disk degeneration.[1] Current treatments for IVD degeneration are generally targeted at the symptoms and are designed to relieve pain and restore some function without treating the problem or repairing the disk directly. In repairing the IVD, the aim is to induce regeneration of the tissue *in situ* via biological manipulation, whereas replacing the IVD requires development of a functional tissue unit *in vitro* and implanting it *in vivo*.[2,3] The physiological properties of the disk are linked to the composition of its extracellular matrix (ECM). Tissue engineering methods tend to focus on techniques directed toward replenishing the ECM of the disk to restore disk function.[4] Using a combination of cells and synthetic or natural biomaterials provides a tissue engineering approach to regenerate the matrix and fully restore normal function to the IVD.

The IVD is comprised of a central, gelatinous nucleus pulposus (NP), surrounded by a fibrous lamellar annulus fibrosus (AF). Both tissues contain an abundant matrix of negatively charged proteoglycans (PGs) entangled with collagen fibers. The AF consists of an ECM composed of both type I and type II collagen oriented in lamellar structures that are rich in type I collagen.[3] Engineering a functional replacement for the AF of the IVD is contingent on recapitulation of the AF structure, composition, and mechanical properties.[5] The AF of the IVD is the load bearing component, and its strength depends on the composition and organization of its ECM.[6]

The matrix of normal NP of the IVD is comprised of an interwoven network of PGs, predominantly aggrecan and collagens (particularly type II collagen, which is characteristic of hyaline cartilage), with embedded chondrocytic cells.[4] IVDs differ from articular cartilage in that they contain a

[1]Department of Biomedical Engineering, Tufts University, Medford, Massachusetts.
[2]Department of Orthopaedic Surgery, University of Tennessee Health Science Center, Memphis, Tennessee.
Departments of [3]Orthopedic Surgery and [4]Molecular Science and Technology, School of Medicine, Ajou University, Suwon, Korea.

significantly higher proportion of PG and versican. Some differences in the structure of PGs in cartilage (large PG aggregates) and the NP (nonaggregated PG monomers) tissues have been observed.[7] However, hyaline cartilage and NP possess similar macromolecules in their ECM and contain PGs that have the ability to interact specifically with collagen molecules.[8] In addition, as with articular cartilage, the disks resist compressive forces due to their high content of PGs and aggrecan in the NP.[9] IVD degeneration by changes in matrix biology, a disruption of the matrix, and a loss of function cause dehydration and loss of hydrophilic properties of the NP matrix (which normally attract water and provide the disk with high swelling pressure that supports the disk height and functions), thus leading to a loss of disk height and eventually to disability and pain.[10,11] Therefore, successful regenerated IVD tissue should achieve anatomic morphologies for both AF and NP tissues, while also restoring the function of both tissues.

Scaffolds for IVD tissue engineering are required to immediately restore functions, whereas seeded cells gradually replace the initial biomaterial with a new, native matrix. The scaffold should also allow maintenance of cell phenotype and be fully biodegradable over time for the full restoration of tissue structure and function.[12] A variety of scaffolds have been used for tissue engineering of the AF of the IVD, including collagen,[13] agarose,[14] collagen-glycosaminoglycan (GAG),[15] alginate-chitosan,[16] and polyglycolic acid (PGA)/polylactic acid (PLA).[17]

Some studies have focused on AF tissue formation by using a lamellar scaffold composed of alginate/chitosan[16] or poly(polycaprolactone triol malate) with demineralized bone matrix gelatin.[5] However, these AF tissues focused on scaffold designs and were not able to reconstruct the entire IVD, including NP tissue, though the scaffolds supported AF cell growth and proliferation. Several studies have reported tissue engineered NP using injectable materials such as collagen,[18,19] alginate,[20] chitosan,[21] fibrin,[22,23] and hyaluronic acid (HA).[24] These injectable scaffolds are preferable for IVD engineering, as they allow needle-guided graft delivery to minimize trauma to the disk.[25] However, these approaches do not regenerate the entire IVD tissue. Therefore, an alternative approach utilizing biphasic scaffolds is an attractive prospect for engineering entire IVD tissue systems.

In previous studies directed toward engineering the entire IVD, a composite IVD was fabricated by using PGA and alginate with two different cell types, to form a tissue with AF and NP components.[17] Methods were developed for the construction of composite structures consisting of AF and NP cells seeded on separate matrices; however, the NP cells in alginate did not accumulate significant levels of ECM, with poor collagen accumulation.[17] A biphasic IVD structure was also formed by using PLA nanofibrous scaffolds and HA gels with bone marrow-derived mesenchymal stem cells (MSCs) for AF and NP tissue regeneration.[26] Although the production of a biphasic cartilaginous tissue construct was reported, the MSC seeded PLA/HA constructs produced AF and NP tissues that were similar in composition due to the use of only chondrogenic media, and lamellar AF morphologies were not pursued.

The goal for regenerating disk tissue is to achieve anatomic morphology and restoration of biological function. Toward this goal, we have previously used porous silk scaffolds for AF tissue regeneration[27,28] and also have shown that silk fibrin/HA composite gels can serve as chondrocyte delivery biomaterials.[29,30]

In the present work, the goal was to design a biphasic scaffold system to support both AF and NP morphologies and cells. We, therefore, utilized a silk and fibrin/HA matrix system and seeded these components with either porcine AF cells or porcine chondrocytes. We determined whether the biphasic structure, consisting of lamellar silk scaffolds (to mimic the AF) with fibrin/HA gel (to mimic the NP), could support the architecture and cell functions of IVD tissue.

Materials and Methods

Isolation and culture of AF and chondrocyte cells

Porcine annulus fibrous cells and chondrocytes were kindly provided by the University of Tennessee Health Science Center (UTHSC). AF cells and chondrocytes were isolated from porcine IVD and articular cartilage, respectively. Briefly, IVDs used in this investigation were obtained from the lumbar disk of newborn porcine (2–3 weeks old, Grade I: macroscopic grading of age). The spine was sectioned between each of the lumbar disks from T10 to L5. The muscles and tendons were removed, and the column was transversally sectioned in the middle of each disk. The surrounding AF was separated from the upper and lower vertebral disks, and the outer section with connection ligaments was discarded. Cells from the AF tissues were isolated by 1–2 h digestion at 37°C in 0.05% pronase (Boehringer Mannheim), followed by overnight digestion at 37°C in 0.2% collagenase (Worthington Biochemicals) by using modified Dulbecco's modified Eagle's medium (DMEM)/F12 medium (Gibco BRL) with 5% fetal calf serum (FCS; Gibco), 4.8 mM $CaCl_2$, and 40 mM HEPES buffer (Sigma-Aldrich). After 18 h of shaking, the completely digested specimens released cells, which was confirmed by phase contrast microscopy. The digested samples were centrifuged at 250 *g* for 5 min to isolate the annulus fibrosis cells for counting.

Pieces of porcine articular cartilage were finely minced and washed with phosphate-buffered saline (PBS). They were then digested in 0.2% (w/v) collagenase (Worthington Biochemical) in PBS for 5 h at 37°C. Using a cell strainer (70 μm Nylon; Falcon), the cells were filtered, pooled, and centrifuged at 1200 rpm for 10 min. After being washed twice with PBS, the cell pellet was resuspended in DMEM (Gibco) supplemented with 10% fetal bovine serum (FBS; Gibco), 100 U/mL penicillin G (Gibco), and 100 μg/mL streptomycin (Gibco).

Both cell types were counted by using a hemacytometer, and cell numbers and viabilities were determined by using a trypan blue exclusion test. The cells were then plated at a density of 1.5×10^5 cells/cm^2 and placed at 37°C in a 5% CO_2 incubator. The DMEM/F12 for AF cells and DMEM for chondrocyte culture medium that included 10% FBS (Gibco), 1% antibiotic-antimycotic (Gibco), and 50 μg/mL ascorbic acid (Sigma) were changed every other day. The primary AF cells and chondrocytes were passaged twice before the experiments.

Silk composite scaffold fabrication

Preparation of silk solution. Silk fibroin (SF) solutions were prepared according to the procedures previously described.[31] Briefly, 6%–8% (w/v) SF solution was prepared from *Bombyx mori* silkworm cocoons. The cocoons were extracted in a 0.02 M Na_2CO_3 solution, dissolved in a 9.3 M

LiBr solution, and subsequently dialyzed against distilled water.

Preparation of lamellar and porous silk toroidal disks for AF. To make lamellar-shaped silk scaffolds, a 1.5 mL aliquot of 4% SF/0.2% sodium alginate mixture solution was added to a silicone mold (12 mm diameter, 5 mm thick) with one side capped with parafilm. Immediately, these molds were placed in a freezer at −80°C for 2 h. Subsequently, the scaffolds were lyophilized for 2 days, and then, water was annealed for 6 h to generate the insoluble state of silk by inducing beta sheet crystallinity.[32] The scaffolds were then submerged in water for 24 h to remove the mixed alginate.

To generate porous scaffolds, no salt was added. Instead, 50 mM carbodiimide (1-3-dimethylaminopropyl 3-ethylcarbodiimide hydrochloride [EDAC]) and 20 mM N-hydroxysuccinimide (NHS) were mixed in 2 mL aliquots of a 4% SF solution that was kept in teflon cylinder containers at room temperature for 2 h. The containers were then placed in a freezer at −80°C for 2 h. Subsequently, the scaffolds were lyophilized for 2 days and removed from the containers. To remove the EDAC/NHS residue, the lyophilized silk sponge was suspended in 10 mL of quenching solution (5:1 mixture of a 0.25 M $NaHSO_3$ solution and 0.5 N H_2SO_4).

Toroidal disk scaffolds were manually formed out of the lamellar and porous structures to generate an outer diameter of 8 mm, an inner diameter of 3.5 mm, and a height of 3 mm by using round, disposable punches (Acuderm, Inc.). Toroidal disks were submerged in 70% EtOH for sterilization in preparation for cell cultivation experiments after washing with distilled water for 1 day. Before cell seeding, the scaffolds were conditioned overnight with the culture medium.

Fibrin/HA gel for NP

To prepare fibrin/HA composite gels, the porcine chondrocyte cells were pelleted by centrifugation, and then resuspended in a solution containing fibrinogen (10 mg/mL; Green Cross) with 1300 kDa HA (10 mg/mL, 6000 cps viscosity, Lifecore).[30] The porcine chondrocyte suspension of 5×10^6 cells/mL was then homogeneously mixed with aprotinin (Green Cross), 60 U/mL thrombin (1000 U/mg protein; Sigma), a fibrin stabilizing Factor XIII, and 50 mM $CaCl_2$. The fibrin/HA mixture (250 μL) was dropped into the central region of the silk lamellar structure or the porous disks, thereby forming a gel.

Cultivation of IVD biphasic gel-silk scaffold structures

To make AF-like tissues, AF cells were seeded on both top and bottom of the toroidal disk scaffolds of the lamellar and porous materials by using static seeding. Cell seeded scaffolds were incubated for 3 h before adding culture medium and then, continuously in AF culture media (DMEM/F12 medium included 10% FBS) for 2 weeks (phase I, Fig. 1a). Porcine chondrocytes were encapsulated in a fibrin/HA hydrogel and embedded in the center of the biphasic construct (phase II, Fig. 1a). AF-NP biphasic IVD constructs were cultured for 4 weeks (AF-NP 4 weeks) subsequent to the initial culture of the AF tissue (AF 2 weeks), for a total of 6 weeks. (Fig. 1a) Each fibrin/HA gel–loaded silk lamellar and porous scaffold was transferred to a six-well culture plate and cultured in chondrogenic defined medium (CDM), consisting of high-glucose DMEM (Gibco) supplemented with 10 ng/mL transforming growth factor-β (TGF-β1) (Peprotech), 1% antibiotic-antimycotic (Gibco), insulin 6.25 μg/mL, selenious

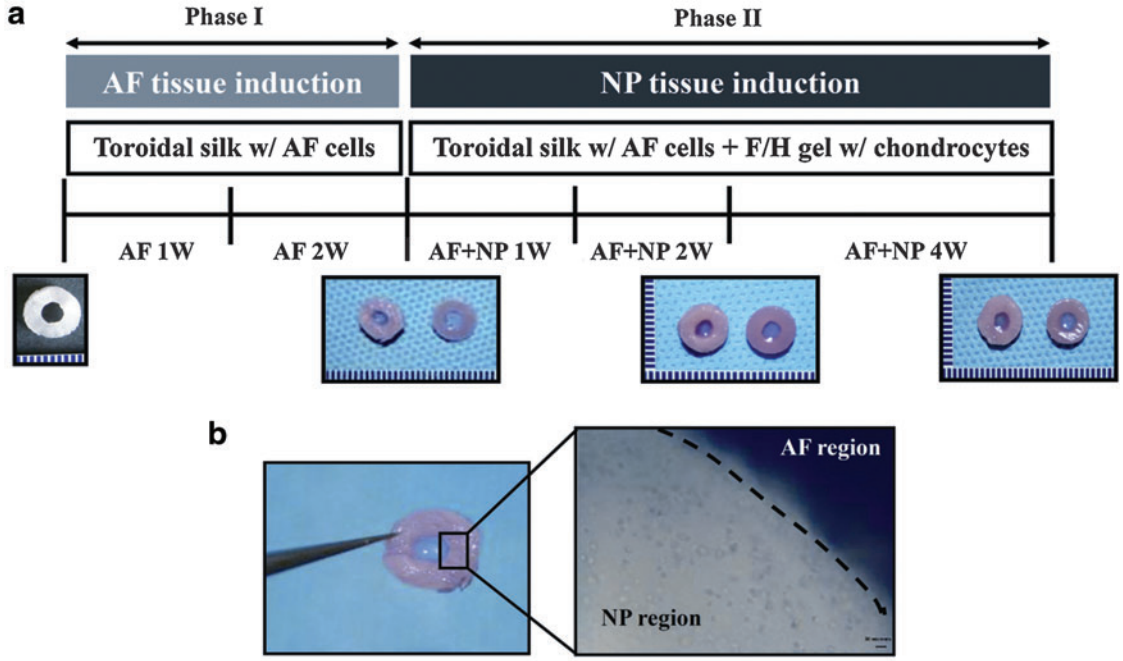

FIG. 1. **(a)** Experimental scheme: nucleus pulposus (NP) tissue differentiation for additional 4 weeks (annulus fibrosus [AF]-NP 4 weeks) after AF tissue induction for 2 weeks (AF 2 weeks), **(b)** biphasic intervertebral disk (IVD) structure (silk scaffold combined with fibrin/hyaluronic acid [HA] gel) using porcine-derived AF cells and chondrocytes. Color images available online at www.liebertonline.com/tea

acid 6.25 μg/mL, transferin 6.25 μg/mL, 50 μg/mL ascorbic acid, 100 nM dexamethasone, 40 μg/mL proline, 1.25 mg/mL bovine serum albumin (BSA), and 100 μg/mL sodium pyruvate. All products were purchased from Sigma-Aldrich.

Scanning electron microscopy for cell proliferation on the structure

The cross-sections of the scaffolds prior/post cell seeding were examined by scanning electron microscopy (SEM, Zeiss FESEM Supra55VP). The samples were fixed for 24 h with 0.4% glutaraldehyde and then dehydrated in a series of graded ethanols before coating with gold/palladium for 3 min before SEM observation.

Cell viability in 3D scaffolds

Viable cells in silk scaffolds and fibrin/HA gels after 2 weeks of the AF-NP coculture (AF-NP 2 weeks) were screened by using a live/dead kit (Molecular Probe). Following the manufacturer's instruction, the *in vitro* sample was treated in a solution for 40 min. The solution is a mixture of three components: 2 mM ethidium homodimer-1, PBS, and 4 mM calcein AM. Washed in sterilized PBS, the sample-embedded slide was observed by a Leica confocal microscope (Wetzlar) with Leica confocal software. The region of interest was selected from z-plane images to include either the surface or the internal pores, beginning with a bottom section at least 1 mm above the surface of the scaffolds. Depth projection micrographs were obtained from 20 horizontal sections imaged at a depth distance of 50 mm from each other. Live cells were visualized green and dead cells, red. Viability of cells was measured by dividing the number of viable cells (green cells) by total cells (green cells + red cells), determined by using Image J.

Histological analysis

After macroscopic observation, tissues were fixed with 4% formalin for 24 h. These were then embedded in paraffin and sectioned in 4-μm-thick slices. Serial sections were stained with hematoxylin and eosin to observe cell/scaffold morphology. To evaluate GAG deposition, sections were stained with 1% alcian blue (Sigma) in 1 N HCl (pH 1.0) for 40 min for alcian blue staining. Immunohistochemistry was also carried out to screen for expression of type I and II collagen as the major ECM protein of IVD. The sections were sequentially washed in 70% ethanol and PBS, treated with 3% H_2O_2 in PBS, and 0.15% Triton X-100 was added. Once blocked with 1% BSA solution, they were reacted with a monoclonal antibody raised against porcine type I and II collagen (1:200; Chemicon) for 1 h, followed by addition of a biotinylated secondary antibody. The protein was then detected by using a horseradish peroxidase-conjugated avidin system (Vector Laboratories). The immunostained sections were counterstained with Mayer's hematoxylin (Sigma) before microscopic examination with a Leica DMIL light microscope (Wetzlar).

Biochemical assays for DNA, GAGs, and collagen content

For chemical analysis of AF (outer diameter of 8 mm, inner diameter of 3.5 mm, and height of 3 mm) and NP (diameter 3.5, height 3 mm) components, the recovered constructs were separated into AF and NP components by using round disposable punches (Acuderm Inc,). The separated samples ($n = 4$) for DNA and GAGs were digested for 16 h with papain solution (125 μg/mL of papain, 5 mM L-cystein, 100 mM Na_2HPO_4, 5 mM EDTA, and pH 6.2) at 60°C.

DNA content was measured by using the PicoGreen DNA Assay according to the manufacturer's protocols (Molecular Probes). After centrifugation, a 25 μL aliquot of supernatant was taken from each sample and placed into 96-well plates with each well containing 75 μL of 1 × TE buffer. A standard curve was generated by using lambda phage DNA in 0, 2.5, 5, and 10 μg/mL concentrations. One hundred microliters of a 1:200 dilution of Quant-iT PicoGreen reagent was added to each well and read by using a flurorimeter with an excitation wavelength of 480 nm and an emission wavelength of 528 nm. Total GAG content was analyzed by using a 1, 9-dimethylmethylene blue (DMB) assay.[33] Individual samples were mixed with the DMB solution, and the absorbance was measured at 525 nm. Total GAG of each sample was extrapolated by using a standard plot of shark chondroitin sulfate (Sigma) in the range of 0–100 μg/mL. The tissue engineered constructs were digested with pepsin solution (1 mg/mL of pepsin, pH 3.0) at 4°C for 48 h to determine total collagen content. Total collagen was measured as we had previously reported.[30] A dye solution (pH 3.5) was prepared with Sirius red dissolved in a picric acid saturated solution (1.3%; Sigma) to a final concentration of 1 mg/mL. The digested samples were dried at 37°C in 96-well plates for 24 h and then reacted with the dye solution for 1 h on a shaker. The samples were then washed five times with 0.01 N HCl, and the dye–sample complex in each well was resolved in 0.1 N NaOH and absorbance was read at 550 nm (Versa MAX; Molecular Devices). Total collagen in each sample was extrapolated by using a standard plot of bovine collagen (Sigma) in the range of 0–500 μg/mL.

Real-time PCR

The recovered constructs were separated into AF and NP components by using round, disposable punches. The separated components ($n = 4$ per group) were transferred into 2 mL plastic tubes, and 1.0 mL of Trizol was added. Scaffolds were chopped with micro scissors on ice. The tubes were centrifuged at 12,000 g for 10 min, and the supernatant was transferred to a new tube. Chloroform (200 μL) was added to the solution and incubated for 5 min at room temperature. Tubes were again centrifuged at 12,000 g for 15 min, and the upper aqueous phase was transferred to a new tube. One volume of 70% ethanol (v/v) was added and applied to an RNeasymini spin column (Qiagen). The RNA was washed and eluted according to the manufacturer's protocol. The RNA samples were reverse transcribed into cDNA by using oligo (dT)-selection according to the manufacturer's protocol (High Capacity cDNA Archive Kit; Applied Biosystems). Collagen type Iα1 (*Col Iα1*), collagen type IIα1 (*Col IIα1*), and aggrecan levels were quantified by using the Mx3000 Quantitative Real Time PCR system (Stratagene).

All data analysis employed the Mx3500 software (Stratagene) based on fluorescence intensity values after normalization with an internal reference dye and baseline correction. Differences of gene expression were analyzed by using the comparative Ct method (Ct [delta][delta] Ct comparison). Ct values for samples were normalized to an endogenous housekeeping gene. PCR conditions were 2 min at 50°C, 10 min at 95°C, and then 50 cycles at 95°C for 15 s, and 1 min

at 60°C. The data were normalized to the expression of the housekeeping gene, glyceraldehyde-3-phosphate-dehydrogenase (*GAPDH*) within the linear range of amplification and differences.[34] The target probes were labeled at the 5′ end with fluorescent dye VIC and with the quencher dye TAMRA at the 3′ end. Primer sequences for the porcine *GAPDH, Col Iα1, Col IIα1,* and *aggrecan* gene are summarized in Table 1. Probes were purchased from Assay on Demand (Applied Biosciences).

Statistical analysis

Statistical differences in biochemical and transcript quantitative analysis were determined by using a Mann–Whitney U test (Independent *t*-test; SPSS) Statistical significance was assigned as $*p < 0.05$, $**p < 0.01$, and $***p < 0.001$, respectively.

Results

Biphasic structure

The experimental scheme, described in Figure 1a, was designed to generate a biphasic construct consisting of an NP-like tissue differentiation for 4 weeks (AF-NP 4 weeks) after an initial AF tissue induction for 2 weeks (AF 2 weeks). Figure 1b shows the biphasic scaffold consisting of AF and NP regions. AF cells were seeded on the toroidal disk scaffolds with the lamellar and porous materials, and then porcine chondrocytes were encapsulated in a fibrin/HA hydrogel and embedded in the center of the toroidal disk for the biphasic construct.

Cell morphology and viability

The seeded porcine AF cells were supported in the lamellar silk scaffolds over 2 weeks. AF cells spread along the lamellar walls, whereas cells seeded on the porous scaffolds showed limited cell populations at the surface of the scaffolds (Fig. 2). SEM revealed that the interlamellar distance in the lamellar scaffolds was 150–250 μm (Fig. 2a), and the average pore sizes of the porous scaffolds were 100–250 μm (Fig. 2d). Cells seeded in the lamellar silk scaffolds showed homogeneous distributions and spread along the lamellar walls after 2 weeks (Fig. 2b, c), whereas cells in the porous scaffolds did not penetrate into the interior and spread more prominently along the surfaces of the scaffolds (Fig. 2e, f). Cell viability was assessed at 2 weeks after AF cells and chondrocyte cocultures (AF-NP 2 weeks). More than 90% of the attached and proliferated AF cells survived in both scaffolds based on live/dead staining. Encapsulated chondrocytes in the fibrin/HA gels also showed good cell survival with both types of scaffold (Fig. 3).

Histology and immunohistochemistry analysis

For the identification of the AF and NP-specific ECM molecules, thin sections of each specimen were stained with alcian blue and antibodies for type I and II collagen at AF-NP 4 weeks. In scaffold sections with alcian blue staining, NP-like tissues generated by fibrin/HA gel with chondrocytes were more intensely stained compared with AF-like tissue generated by silk scaffolds with AF cells (Fig. 4a, e). Importantly, lamellar silk scaffolds showed better integration between the AF and gel for the NP, whereas the porous scaffolds had a more separated border between the NP and AF regions (Fig. 4b, f). From the type I collagen staining, cells in the AF regions stained positive for ECM constituents of AF tissue in both types of scaffolds. However, type I collagen staining was homogeneous and distributed within the entire area of the lamellar structures, whereas the porous scaffolds showed positive staining mostly at the surface (Fig. 4c, g). In addition, cultured NP-like tissue in the lamellar scaffolds stained through large areas for type II collagen (arrows) compared with the porous scaffolds (Fig. 4d, h).

DNA, GAGs, and collagen content

The DNA content of the AF-like tissue, in both the lamellar and porous scaffolds, increased slightly over time. However, in the lamellar scaffolds, the value was significantly higher than the porous silk scaffolds through 4 weeks of culture (Fig. 5a). In addition, the lamellar silk scaffolds showed increasing GAGs and collagen synthesis throughout the culture period. The GAG content of the lamellar silk scaffold was two times higher than the porous scaffolds at AF-NP 4 weeks. The amounts of GAGs (μg/mg construct) in the lamellar and porous silk scaffolds were 5.9 ± 1.3 and 2.9 ± 0.2, respectively ($p < 0.001$) (Fig. 5b). The total collagen content (4.1 ± 0.7 μg/mg construct) in the lamellar silk scaffold was 1.7 times higher than the value in the porous scaffold (2.4 ± 0.2) at the same time point (Fig. 5c).

The DNA content of the cultured NP-like tissues in the fibrin/HA gels within the lamellar silk AF scaffolds was significantly higher at AF-NP 4 weeks than the fibrin/HA gels within the porous outer silk structures (Fig. 6a). Although GAG content in the NP regions of both scaffolds increased with time, NP regions in the lamellar scaffolds were statistically higher with regard to GAG synthesis than in the porous scaffolds at AF-NP 4 weeks (Fig. 6b). Total collagen content

Table 1. PCR Primer Pairs Used for Detection of Three Target Genes and a Housekeeping Gene

Gene	*Primer sequence (5′ > 3′)*	*Probe*
Aggrecan	F: CCCAACCAGCCTGACAACTT R: CCTTCTCGTGCCAGATCATCA	ACGCAGTCCTCTCCAGTGGCGAA
Col Iα1	F: AGAAGAAGACATCCCACCAGTCA R: AGATCACGTCATCGCACAACA	AACGGCCTCAGGTACCATGACCGA
Col IIα1	F: CAGGTGAAGGTGGGAAACCA R: ACCCACGAGGCCAGGA	ATCAGGGCGTTCCTGGTGAAGCTG
GAPDH	F: TCGGAGTGAACGGATTTGG R: CCAGAGTTAAAAGCAGCCCT	CGCATCGGGCGCCTGGTC

Col Iα1, collagen type Iα1; Col IIα1, collagen type IIα1.

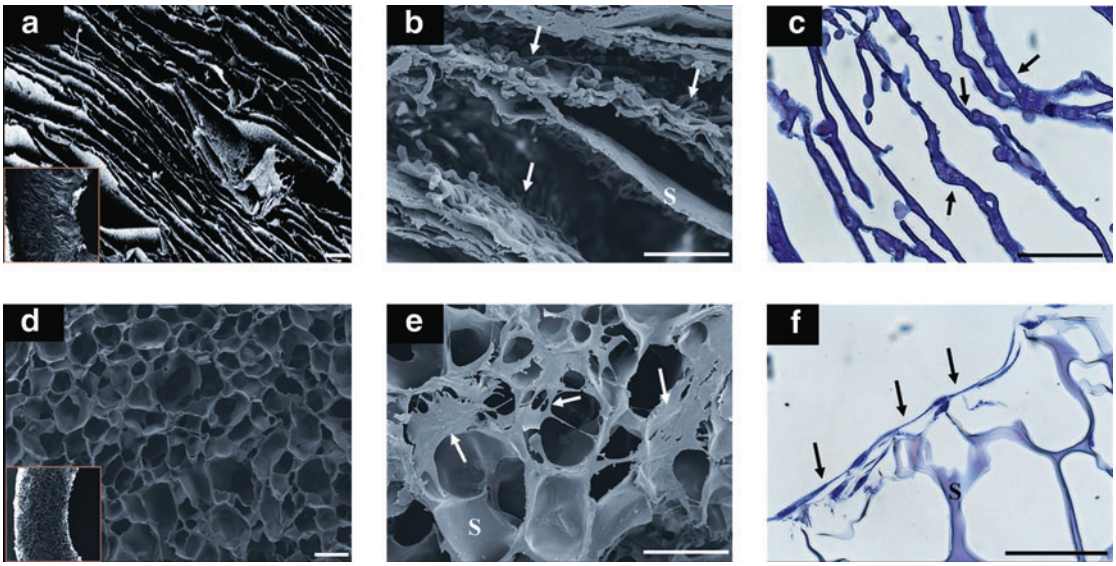

FIG. 2. SEM images of lamellar and porous scaffolds **(a)** lamellar scaffolds **(b)** porcine AF cells on lamellar at AF-2 weeks, **(d)** porous scaffolds, **(e)** porcine AF cells on porous scaffolds at AF-2 weeks. H&E staining for cells: **(c)** lamellar scaffolds, **(f)** porous scaffolds. Scale bars = 200 μm. Arrows indicate cells on the scaffolds, and S indicates silk. Color images available online at www.liebertonline.com/tea

was significantly higher in the NP regions of the lamellar scaffolds at AF-NP 2 weeks, whereas both groups did not show statistical differences at AF-NP 4 weeks (Fig. 6c).

Real-time PCR analysis

Transcript levels related to AF differentiation markers (*Col Iα1* and *aggrecan*) and NP differentiation markers (*Col IIα1* and *aggrecan*) were analyzed by real-time RT-PCR and normalized to *GAPDH* within the linear range of amplification. At AF-NP 4 weeks, the mRNA levels of *Col Iα1* and aggrecan in the AF regions were significantly higher (around two times) in the lamellar silk scaffold compared with the porous scaffold (Fig. 7a, b). On the other hand, the mRNA levels of the *Col IIα1* gene in the NP regions were also significantly higher in the lamellar silk scaffold compared with the porous silk scaffold, whereas aggrecan gene expression did not show statistical differences between the two scaffold types (Fig. 7a, c).

Discussion

Studies on tissue engineered IVDs are not common due to the complexity of the system.[35] A key component for such

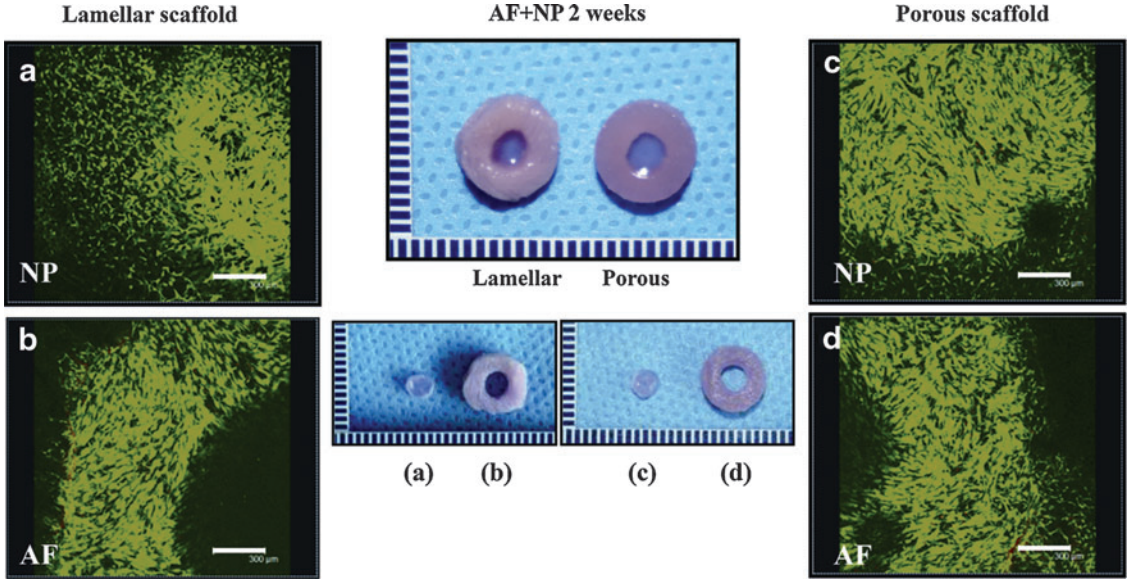

FIG. 3. Live/dead staining of cells in biphasic structures of both silk scaffolds (porcine AF cells) and fibrin/HA gel (porcine chondrocytes) at AF-NP 2 weeks: **(a)** fibrin/HA gel in the center of lamellar AF, **(b)** lamellar AF scaffold, **(c)** fibrin/HA gel in the center of porous AF scaffold, and **(d)** porous AF scaffold. Scale bars = 300 μm. Color images available online at www.liebertonline.com/tea

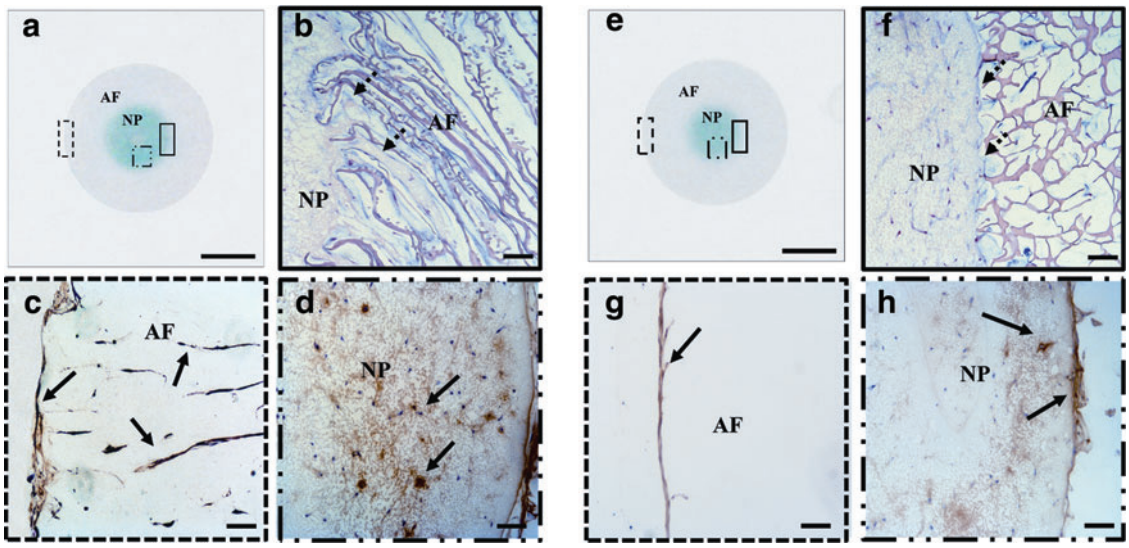

FIG. 4. Histological and immunohistochemical staining of biphasic structures at AF-NP 4 weeks. Lamellar scaffold: **(a)** alcian blue staining of entire structure, **(b)** hematoxylin and eosin (H&E) staining of merged region between AF and NP, **(c)** type I collagen staining of lamellar scaffolds, **(d)** type II collagen staining of fibrin/HA gel. Porous scaffold: **(e)** alcian blue staining of entire structure, **(f)** H&E staining of merged area between AF and NP, **(g)** type I collagen staining of porous scaffold, **(h)** type II collagen staining of fibrin/HA gel. Extracellular matrix stained positive for type I and II collagen with brown color (solid arrows). Dash arrows indicate integration area between silk scaffolds for AF and gel for NP. (A, E) scale bars = 3 mm, **(b, c, d, f, g, h)** scale bars = 100 μm. The dotted rectangle furthest to the left is shown in the bottom left (**c** and **g**). The other dotted rectangle is shown in the bottom right (**d** and **h**) and the solid rectangle is shown in top right (**b** and **f**). Color images available online at www.liebertonline.com/tea

tissues is the biomaterial matrix utilized to support structure and function with appropriate cell types. The scaffold is a functional template that guides cellular remodeling.[36] The scaffold can function as a delivery vehicle for cells.[4] The physical and chemical requirements of scaffolds for cell/tissue ingrowth include biocompatibility, support for cell growth, retention of differentiated cell functions, biodegradability, and uniformly distributed and interconnected pore structures to provide adequate transport and cell migration during ECM production.[37]

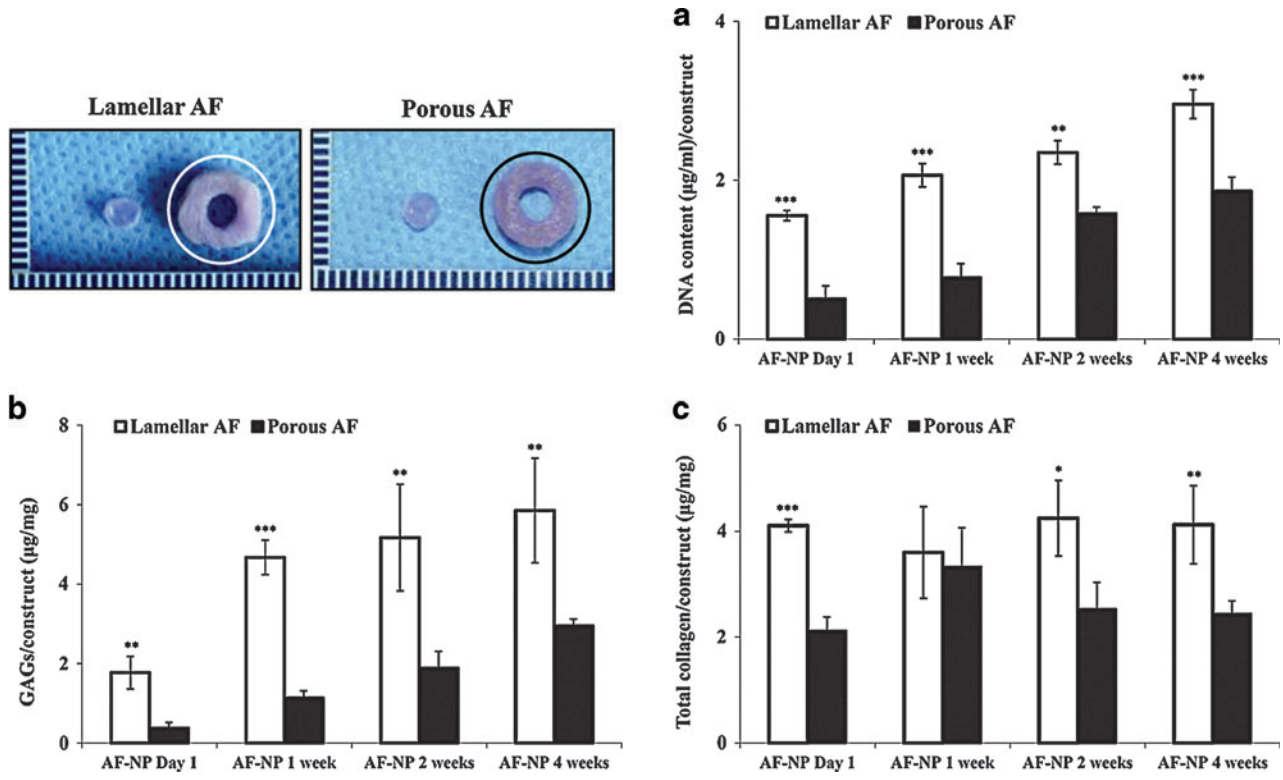

FIG. 5. Chemical analysis of silk scaffolds of AF region at AF-NP 4 weeks: **(a)** DNA content, **(b)** GAGs, **(c)** total collagen content per construct. Data shown as mean ± standard deviation, 4 samples (*$p < 0.05$, **$p < 0.01$, and ***$p < 0.001$). GAGs, glycosaminoglycans. Color images available online at www.liebertonline.com/tea

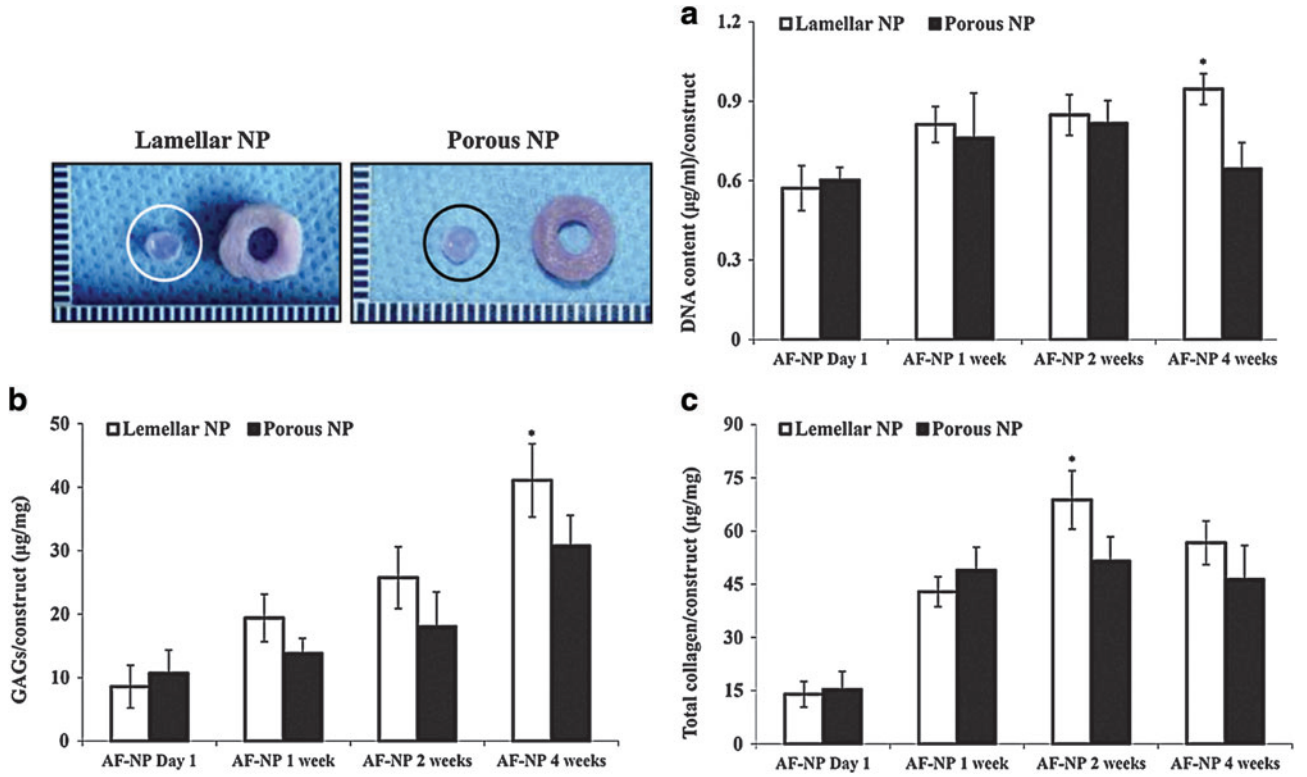

FIG. 6. Chemical analysis of fibrin/HA gel of NP region at AF-NP 4 weeks: **(a)** DNA content, **(b)** GAGs, **(c)** total collagen content per construct. Statistically significant differences, $n = 4$ (*$p < 0.05$). Color images available online at www.liebertonline.com/tea

Various biomaterials have been explored for AF tissue replacement.[13,15–17] Silk scaffolds have shown potential for bone and cartilage tissue engineering *in vitro* and *in vivo* due to their impressive mechanical properties, biocompatibility, and biodegradability.[31,38] Two types of scaffold morphologies were investigated in the current work, both formed from silk. The first mimicked the lamellar features of the AF of native IVD, whereas the second was a porous spongy scaffold to serve as a control. Toroidal scaffolds were formed with appropriate interlamellar spacing and structure. The porous silk scaffolds have previously been used for AF tissue engineering.[27,28] However, tissue in-growth was limited and not uniformly distributed throughout the scaffold.[27] In addition, although AF tissue formation and better cell distribution in porous silk scaffolds were enhanced when grown in dynamic spinner flasks, the lamellar AF structure was not mimicked.[28]

Therefore, in the current study, lamellar structures were generated by a simple freeze-drying technique to recapitulate the native AF structure. The target interlamellar wall distance (150–250 μm) used in this study was generated by mixing a silk solution with an approximately 0.2% sodium alginate solution before freeze drying. The engineered lamellar scaffolds supported cell seeding and proliferation to form an AF-like tissue due to cells penetrating along the walls from the outside to the inside of the scaffold. In contrast, porous silk scaffolds showed only proliferating cells on the surface of the scaffolds (Fig. 2). Low cell penetration on the porous silk scaffold was previously reported; scaffolds with 150–250 μm pores showed a nonuniform distribution of

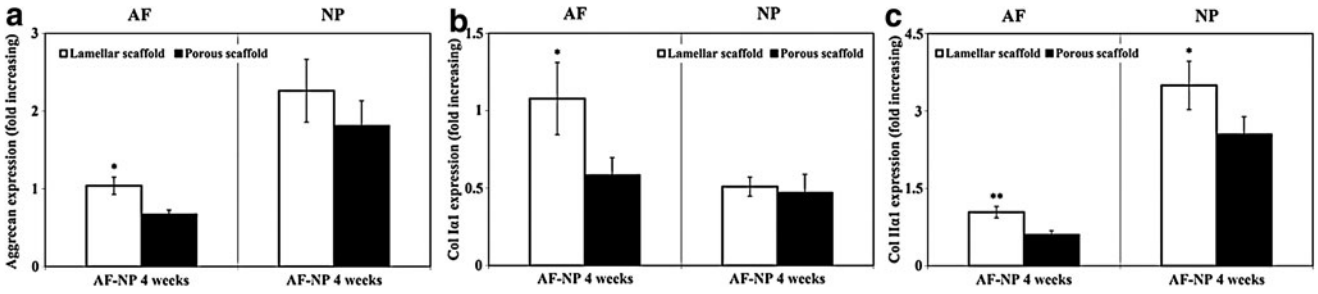

FIG. 7. Transcript levels related to IVD tissue differentiation markers at AF-NP 4 weeks: **(a)** *aggrecan*, **(b)** collagen type Iα1 (*Col Iα1*), and **(c)** collagen type IIα1 (*Col IIα1*). Data quantified by real-time PCR and normalized to *GAPDH* within the linear range of amplification. Data are shown as mean ± standard deviation from N = 4, *$p < 0.05$ and **$p < 0.01$.

tissue growth.[27] It appears that the AF tissue mimicking lamellar silk structures can serve as a structural guide for more homogeneous cell distribution. In addition to supporting cell proliferation, it is critical to achieve good integration between the separate regions of the tissue. Excellent integration between AF and NP regions was found in the lamellar system (Fig. 4b) when compared with the porous silk scaffold (Fig. 4f); a transition zone similar to native IVD tissue was generated in these lamellar systems, even though two different types of cells and materials were used for each region. However, based on our scaffold preparation method, the lamellar structures were not circumferentially oriented. Circumferentially oriented structures are assumed to be important for the functional restoration of AF tissue. Therefore, development of further methods will be needed to fully recapitulate this complex architecture.

IVD tissue should be mechanically stable to fatigue failure, especially when the bending moment is high.[39] The mechanical property of the human AF tissue is reported at 7.2–27.2 MPa for tensile modulus and 1.23 MPa for compressive modulus.[40–42] In our previous study, silk scaffolds with lamellar structure exhibited 0.26 MPa for tensile modulus and 164.80 kPa for compressive modulus, whereas silk scaffolds with a porous structure showed 1.30–1.41 MPa for tensile modulus and 293.78–347.58 kPa for compressive modulus.[32] Even though the mechanics of general silk scaffolds are lower than native IVD tissues, new strategies have been sought to enhance silk biomaterial mechanical properties, for example, by reinforcing silk sponges with silk particles (up to 1.93 MPa for compressive modulus).[43,44] Thus, further researches aiming toward improved mechanically properties with these scaffolds will be needed before exploration of *in vivo* studies.

Although many researchers have focused on the AF, the NP also contains a network of elastic fibers with a distinct architecture.[45] An injectable biomaterial is potentially useful for the restoration of NP disk volume removed during discectomy and for preventing loss of disk height.[46] Flowable materials may be injected via a small incision, thus allowing minimally invasive access to the NP space. Fluids can interdigitate with the irregular surgical defects and may, depending on the material used, physically bond to the adjacent tissue. Injectable biomaterials allow for incorporation and uniform dispersion of cells and/or therapeutic agents.[47] Fibrin and HA composite gels were utilized for NP tissue regeneration in the current study as an injectable gel. Fibrin is an attractive candidate as a natural scaffold polymer, because it can be generated from human plasma and has a good biocompatibility as a wound adhesive.[37] HA is a nonsulfated GAG that constitutes a large proportion of cartilaginous ECM. Two or more polymers can be combined into gels to utilize the benefits of each component, such as fibrin–alginate,[48] HA–alginate,[49] and collagen–fibrin.[50] These previous studies demonstrated the capability of combined matrix gels to support cell proliferation without loss of chondrogenic potential. We have also previously suggested fibrin/HA composite gels as scaffold matrices for chondrogenesis *in vitro* and *in vivo*; transplantation of chondrocytes in these gel systems showed progress in the repair of full-thickness cartilage defects in articular cartilage.[29,30] Although a number of studies have documented the culture of NP cells in alginate as a preferred system due to ease of use and cell retrieval,[17] in this study, fibrin/HA gels were used for cultivating chondrocytes, thus ultimately showing better cell proliferation and GAG synthesis than those previously attained in alginate gels alone.[51] In addition, fibrin/HA composite gels provided appropriate mechanical properties, supported uniform cell distributions, and can be easily prepared with tunable properties.[52]

Progress in research on tissue engineered IVD has been slow because of the complexities involved in cultivating NP cells.[53] There is a need to increase NP cell viability because of their low cell yield from IVDs during harvest and low proliferative capacity. Although the avascular nature of the disk may make the NP an immunologically privileged site and, therefore, make the use of allogeneic cells a tempting proposition, the risk of transferring infectious agents remains real.[54] Therefore, some experiments have been conducted by using chondrocytes as an alternative cell source.[55,56] In addition, within the NP, rounded chondrocyte-like cells are embedded in a random network of type II collagen and aggrecan, supplemented with other PGs, including versican.[57,58] The NP of the IVD is similar to hyaline cartilage over time during development and maturation, expressing markers of chondrocytes such as collagen type II, collagen type IX, aggrecan, and SOX 9.[59] Thus, we used chondrocytes for NP tissue differentiation in the current study. In addition, AF cells from young porcine are used for AF tissue, because it is easy to obtain numerous healthy numbers of AF cells. In our previous study about the aging of IVDs, we observed that the numbers of cells dramatically decreased with aging in AF tissue.[60] The outer AF contains fibroblast-like cells that are elongated and position themselves parallel to the predominant collagen fibril orientation.[61] Therefore, to achieve the biphasic structure, AF cells were seeded in silk scaffolds for AF tissue, and chondrocytes were encapsulated in the fibrin/HA gel for the NP tissue. The cells and biomaterials were cultured in CDM for the NP tissue differentiation for an additional 4 weeks after AF tissue induction with an AF cell culture medium for the initial 2 weeks (Fig. 1a).

The importance of environmental factors in the induction of cell differentiation toward tissue specific outcomes has been emphasized. Due to the low cellular activity and nutrition-deprived environment in degenerated IVDs, it may be necessary to employ growth factors (GFs) for tissue engineering strategies to be more effective.[4] Several GFs have been shown to positively modulate the metabolism of IVD cells: TGF-β, insulin-like growth factor-1, and platelet-derived growth factor stimulate cell proliferation and PG synthesis *in vitro*.[62–64] Among them, TGF-β1 was included in CDM to achieve NP-like tissue. Treatment with TGF-β1 stimulated new ECM synthesis in old or degenerated disks.[64] In addition, TGF-β1 was the optimal GF for stimulating GAG synthesis with both NP and AF cells[65] and increased PG synthesis and cell proliferation when cultured without FBS.[66] In the current study, fibrin/HA composite gels with chondrocytes induced NP tissue features when cultured in CDM including TGF-β1.

A successful scaffold provides physical support for cell attachment and promotes cell proliferation and desired ECM deposition.[16] The major components of the AF ECM are fibrillar collagens and PGs. The largest and most important PG in the disk matrix is aggrecan, which consists of a protein core with attached GAGs.[67] When AF cells were seeded onto

silk lamellar or porous scaffolds, AF cells adhered to both scaffolds and synthesized collagen and PGs. The lamellar scaffolds supported more AF tissue-specific features, based on histological, biochemical, and gene expression data for collagen and aggrecan. In addition, the composite gel combined with lamellar silk scaffold showed significantly higher ECM synthesis and gene expression than the porous silk scaffold control (Figs. 5–7). In particular, AF cells maintained their viability and function during 2 weeks in AF-NP biphasic IVD construct culture after an initial 2 week culture of the AF tissue alone (Fig. 3).

The lamellar silk AF scaffolds were superior to the porous silk AF scaffolds in promoting integration with the fibrin/HA NP gel scaffold. The lamellar AF structure combined with the fibrin/HA gel to mimic the native IVD structure and supported NP tissue growth and proliferation based on histological and biochemical characteristics with gene expression of collagen and aggrecan. These results correlate with the stability of the fibrin/HA gel in lamellar or porous silk scaffolds because of the improved chondrogenesis as shown in our previous study.[68] Chondrocyte activities are maintained only in a proper 3D environment.[69] This cell–matrix interaction is essential for chondrocyte proliferation, differentiation, or survival. For example, cells adhere and interact with their extracellular environment via integrons, and their ability to activate associated downstream signaling pathways depends on the character of the adhesion complexes formed between cells and their ECM, various factors (glucose, oxygen, and cytokines) that are important parameters affecting chondrocyte metabolism.[70] Therefore, a specific cell environment would be a key determinant of cartilage formation. In particular, material degradation is essential in many small- and large-molecule release application and in functional tissue regeneration.[71] Fibrin rapidly degrades and shrinks with chondrocyte culture.[72] In our previous study, fibrin/HA composite gels also showed a lack of complete cartilage formation in peripheral areas of the biomaterials, likely due to inefficient differentiation of cells or the fast degradation of the biomaterials.[30] Although fibrin/HA gel showed potential as a cell delivery vehicle for chondrogenesis, the weak mechanical properties and rapid degradation remain problematic for some applications. However, it is important that the rate of ECM synthesis and degradation be matched and kept in an equilibrium in cartilage tissue engineering.[73] Better chondrogenesis was observed in stable fibrin/HA gel in our previous studies.[29,68] Other studies also showed that long-term stable fibrin gels in combination with scaffolds results increased cellular proliferation while maintaining production of ECM.[74,75] In the current study, lamellar silk scaffolds supported the synthesis of chondrogenic ECM over the entire NP region (Fig. 4). One reason for this outcome is the integration between the lamellar structure of the AF and NP regions compared with porous scaffolds that would facilitate the stability of fibrin/HA gel as a cell environment for differentiation of the NP tissue.

Conclusions

This article describes the fabrication of a biphasic IVD structure by using techniques of tissue engineering. Two different cell types, AF and chondrocyte, were seeded onto a biphasic scaffold composed of lamellar or porous silk scaffolds and fibrin/HA gel, to generate the AF and NP-like tissues. The results demonstrated that tissue-engineered IVD grown on lamellar silk scaffolds with fibrin/HA gel supported improved integration of the two components and improved markers of the tissue types when compared with those grown on porous scaffolds with the fibrin/HA gel. Thus, this original tissue mimicking biphasic scaffold designed to simulate both AF and NP tissues was effective in the formation of an entire artificial IVD unit *in vitro*. This tissue construct could potentially be used as a model system for the study of the native IVD tissue. With additional focus on mechanical requirements, these systems may be useful for future tissue replacements for degenerated IVD.

Acknowledgment

This project was supported by the NIH Tissue Engineering Resource Center (EB002520) and NIH EB003210.

Disclosure Statement

No competing financial interests exist.

References

1. Martin, M.D., Boxell, C.M., and Malone, D.G. Pathophysiology of lumbar disc degeneration: a review of the literature. Neurosurg Focus **13,** E1, 2002.
2. Richardson, S.M., and Hoyland, J.A. Stem cell regeneration of degenerated intervertebral discs: current status. Curr Pain Headache Rep **12,** 83, 2008.
3. Richardson, S.M., Mobasheri, A., Freemont, A.J., and Hoyland, J.A. Intervertebral disc biology, degeneration and novel tissue engineering and regenerative medicine therapies. Histol Histopathol **22,** 1033, 2007.
4. O'Halloran, D.M., and Pandit, A.S. Tissue-engineering approach to regenerating the intervertebral disc. Tissue Eng **13,** 1927, 2007.
5. Wan, Y., Feng, G., Shen, F.H., Laurencin, C.T., and Li, X. Biphasic scaffold for annulus fibrosus tissue regeneration. Biomaterials **29,** 643, 2008.
6. Broberg, K.B. On the mechanical behaviour of intervertebral discs. Spine **8,** 151, 1983.
7. Buckwalter, J.A., Smith, K.C., Kazarien, L.E., Rosenberg, L.C., and Ungar, R. Articular cartilage and intervertebral disc proteoglycans differ in structure: an electron microscopic study. J Orthop Res **7,** 146, 1989.
8. Sztrolovics, R., Grover, J., Cs-Szabo, G., Shi, S.L., Zhang, Y., Mort, J.S., and Roughley, P.J. The characterization of versican and its message in human articular cartilage and intervertebral disc. J Orthop Res **20,** 257, 2002.
9. Hutton, W.C., Ganey, T.M., Elmer, W.A., Kozlowska, E., Ugbo, J.L., Doh, E.S., and Whitesides, T.E., Jr. Does long-term compressive loading on the intervertebral disc cause degeneration? Spine **25,** 2993, 2000.
10. Sebastine, I.M., and Williams, D.J. Current developments in tissue engineering of nucleus pulposus for the treatment of intervertebral disc degeneration. Conf Proc IEEE Eng Med Biol Soc **2007,** 6401, 2007.
11. Urban, J.P., and McMullin, J.F. Swelling pressure of the intervertebral disc: influence of proteoglycan and collagen contents. Biorheology **22,** 145, 1985.
12. Richardson, S.M., Walker, R.V., Parker, S., Rhodes, N.P., Hunt, J.A., Freemont, A.J., and Hoyland, J.A. Intervertebral disc cell-mediated mesenchymal stem cell differentiation. Stem Cells **24,** 707, 2006.

13. Sato, M., Asazuma, T., Ishihara, M., Kikuchi, T., Masuoka, K., Ichimura, S., Kikuchi, M., Kurita, A., and Fujikawa, K. An atelocollagen honeycomb-shaped scaffold with a membrane seal (ACHMS-scaffold) for the culture of annulus fibrosus cells from an intervertebral disc. J Biomed Mater Res A **64,** 248, 2003.
14. Gruber, H.E., Hoelscher, G.L., Leslie, K., Ingram, J.A., and Hanley, E.N., Jr. Three-dimensional culture of human disc cells within agarose or a collagen sponge: assessment of proteoglycan production. Biomaterials **27,** 371, 2006.
15. Rong, Y., Sugumaran, G., Silbert, J.E., and Spector, M. Proteoglycans synthesized by canine intervertebral disc cells grown in a type I collagen-glycosaminoglycan matrix. Tissue Eng **8,** 1037, 2002.
16. Shao, X., and Hunter, C.J. Developing an alginate/chitosan hybrid fiber scaffold for annulus fibrosus cells. J Biomed Mater Res A **82,** 701, 2007.
17. Mizuno, H., Roy, A.K., Vacanti, C.A., Kojima, K., Ueda, M., and Bonassar, L.J. Tissue-engineered composites of anulus fibrosus and nucleus pulposus for intervertebral disc replacement. Spine **29,** 1290, 2004.
18. Sakai, D., Mochida, J., Iwashina, T., Watanabe, T., Suyama, K., Ando, K., and Hotta, T. Atelocollagen for culture of human nucleus pulposus cells forming nucleus pulposus-like tissue *in vitro*: influence on the proliferation and proteoglycan production of HNPSV-1 cells. Biomaterials **27,** 346, 2006.
19. Sakai, D., Mochida, J., Yamamoto, Y., Nomura, T., Okuma, M., Nishimura, K., Nakai, T., Ando, K., and Hotta, T. Transplantation of mesenchymal stem cells embedded in Atelocollagen gel to the intervertebral disc: a potential therapeutic model for disc degeneration. Biomaterials **24,** 3531, 2003.
20. Mizuno, H., Roy, A.K., Zaporojan, V., Vacanti, C.A., Ueda, M., and Bonassar, L.J. Biomechanical and biochemical characterization of composite tissue-engineered intervertebral discs. Biomaterials **27,** 362, 2006.
21. Mwale, F., Iordanova, M., Demers, C.N., Steffen, T., Roughley, P., and Antoniou, J. Biological evaluation of chitosan salts cross-linked to genipin as a cell scaffold for disk tissue engineering. Tissue Eng **11,** 130, 2005.
22. Sha'ban, M., Yoon, S.J., Ko, Y.K., Ha, H.J., Kim, S.H., So, J.W., Idrus, R.B., and Khang, G. Fibrin promotes proliferation and matrix production of intervertebral disc cells cultured in three-dimensional poly(lactic-co-glycolic acid) scaffold. J Biomater Sci Polym Ed **19,** 1219, 2008.
23. Gruber, H.E., Leslie, K., Ingram, J., Norton, H.J., and Hanley, E.N. Cell-based tissue engineering for the intervertebral disc: *in vitro* studies of human disc cell gene expression and matrix production within selected cell carriers. Spine J **4,** 44, 2004.
24. Cloyd, J.M., Malhotra, N.R., Weng, L., Chen, W., Mauck, R.L., and Elliott, D.M. Material properties in unconfined compression of human nucleus pulposus, injectable hyaluronic acid-based hydrogels and tissue engineering scaffolds. Eur Spine J **16,** 1892, 2007.
25. Leung, V.Y., Chan, D., and Cheung, K.M. Regeneration of intervertebral disc by mesenchymal stem cells: potentials, limitations, and future direction. Eur Spine J **15,** S406, 2006.
26. Nesti, L.J., Li, W.J., Shanti, R.M., Jiang, Y.J., Jackson, W., Freedman, B.A., Kuklo, T.R., Giuliani, J.R., and Tuan, R.S. Intervertebral disc tissue engineering using a novel hyaluronic acid-nanofibrous scaffold (HANFS) amalgam. Tissue Eng Part A **14,** 1527, 2008.
27. Chang, G., Kim, H.J., Kaplan, D., Vunjak-Novakovic, G., and Kandel, R.A. Porous silk scaffolds can be used for tissue engineering annulus fibrosus. Eur Spine J **16,** 1848, 2007.
28. Chang, G., Kim, H.J., Vunjak-Novakovic, G., Kaplan, D.L., and Kandel, R. Enhancing annulus fibrosus tissue formation in porous silk scaffolds. J Biomed Mater Res A **92,** 43, 2010.
29. Park, S.H., Cui, J.H., Park, S.R., and Min, B.H. Potential of fortified fibrin/hyaluronic acid composite gel as a cell delivery vehicle for chondrocytes. Artif Organs **33,** 439, 2009.
30. Park, S.H., Park, S.R., Chung, S.I., Pai, K.S., and Min, B.H. Tissue-engineered cartilage using fibrin/hyaluronan composite gel and its *in vivo* implantation. Artif Organs **29,** 838, 2005.
31. Kim, H.J., Kim, U.J., Leisk, G.G., Bayan, C., Georgakoudi, I., and Kaplan, D.L. Bone regeneration on macroporous aqueous-derived silk 3-D scaffolds. Macromol Biosci **7,** 643, 2007.
32. Mandal, B.B., Park, S.H., Gil, E.S., and Kaplan, D.L. Multilayered silk scaffolds for meniscus tissue engineering. Biomaterials **32,** 639, 2011.
33. Whitley, C.B., Ridnour, M.D., Draper, K.A., Dutton, C.M., and Neglia, J.P. Diagnostic test for mucopolysaccharidosis. I. Direct method for quantifying excessive urinary glycosaminoglycan excretion. Clin Chem **35,** 374, 1989.
34. Kim, H.J., Kim, U.J., Vunjak-Novakovic, G., Min, B.H., and Kaplan, D.L. Influence of macroporous protein scaffolds on bone tissue engineering from bone marrow stem cells. Biomaterials **26,** 4442, 2005.
35. Raghunath, J., Rollo, J., Sales, K.M., Butler, P.E., and Seifalian, A.M. Biomaterials and scaffold design: key to tissue-engineering cartilage. Biotechnol Appl Biochem **46,** 73, 2007.
36. Diwan, A.D., Parvataneni, H.K., Khan, S.N., Sandhu, H.S., Girardi, F.P., and Cammisa, F.P., Jr. Current concepts in intervertebral disc restoration. Orthop Clin North Am **31,** 453, 2000.
37. Hubbell, J.A. Materials as morphogenetic guides in tissue engineering. Curr Opin Biotechnol **14,** 551, 2003.
38. Hofmann, S., Knecht, S., Langer, R., Kaplan, D.L., Vunjak-Novakovic, G., Merkle, H.P., and Meinel, L. Cartilage-like tissue engineering using silk scaffolds and mesenchymal stem cells. Tissue Eng **12,** 2729, 2006.
39. Aubin, C.E., Goussev, V., and Petit, Y. Biomechanical modelling of segmental instrumentation for surgical correction of 3D spinal deformities using Euler-Bernoulli thin-beam elastic deformation equations. Med Biol Eng Comput **42,** 216, 2004.
40. Green, T.P., Adams, M.A., and Dolan, P. Tensile properties of the annulus fibrosus. Eur Spine J **2,** 209, 1993.
41. Iatridis, J.C., MaClean, J.J., and Ryan, D.A. Mechanical damage to the intervertebral disc annulus fibrosus subjected to tensile loading. J Biomech **38,** 557, 2005.
42. Schroeder, Y., Elliott, D.M., Wilson, W., Baaijens, F.P., and Huyghe, J.M. Experimental and model determination of human intervertebral disc osmoviscoelasticity. J Orthop Res **26,** 1141, 2008.
43. Rockwood, D.N., Gil, E.S., Park, S.H., Kluge, J.A., Grayson, W., Bhumiratana, S., Rajkhowa, R., Wang, X., Kim, S.J., Vunjak-Novakovic, G., and Kaplan, D.L. Ingrowth of human mesenchymal stem cells into porous silk particle reinforced silk composite scaffolds: An *in vitro* study. Acta Biomater **7,** 144, 2011.
44. Rajkhowa, R., Gil, E.S., Kluge, J., Numata, K., Wang, L., Wang, X., and Kaplan, D.L. Reinforcing silk scaffolds with silk particles. Macromol Biosci **10,** 599, 2010.
45. Urban, J.P., and Roberts, S. Degeneration of the intervertebral disc. Arthritis Res Ther **5,** 120, 2003.

46. Furderer, S., Anders, M., Schwindling, B., Salick, M., Duber, C., Wenda, K., Urban, R., Gluck, M., and Eysel, P. Vertebral body stenting. A method for repositioning and augmenting vertebral compression fractures. Orthopade **31,** 356, 2002.
47. Boyd, L.M., and Carter, A.J. Injectable biomaterials and vertebral endplate treatment for repair and regeneration of the intervertebral disc. Eur Spine J **15,** S414, 2006.
48. Perka, C., Arnold, U., Spitzer, R.S., and Lindenhayn, K. The use of fibrin beads for tissue engineering and subsequential transplantation. Tissue Eng **7,** 359, 2001.
49. Yoon, D.M., Curtis, S., Reddi, A.H., and Fisher, J.P. Addition of hyaluronic acid to alginate embedded chondrocytes interferes with IGF-1 signaling in vitro and in vivo. Tissue Eng Part A **15,** 3449, 2009.
50. Perka, C., Schultz, O., Lindenhayn, K., Spitzer, R.S., Muschik, M., Sittinger, M., and Burmester, G.R. Joint cartilage repair with transplantation of embryonic chondrocytes embedded in collagen-fibrin matrices. Clin Exp Rheumatol **18,** 13, 2000.
51. Stern, S., Lindenhayn, K., Schultz, O., and Perka, C. Cultivation of porcine cells from the nucleus pulposus in a fibrin/hyaluronic acid matrix. Acta Orthop Scand **71,** 496, 2000.
52. Eyrich, D., Gopferich, A., and Blunk, T. Fibrin in tissue engineering. Adv Exp Med Biol **585,** 379, 2006.
53. Gruber, H.E., Stasky, A.A., and Hanley, E.N., Jr. Characterization and phenotypic stability of human disc cells *in vitro*. Matrix Biol **16,** 285, 1997.
54. Mwale, F., Roughley, P., and Antoniou, J. Distinction between the extracellular matrix of the nucleus pulposus and hyaline cartilage: a requisite for tissue engineering of intervertebral disc. Eur Cell Mater **8,** 58, 2004.
55. Kim, A.J., Adkisson, H.D., Wendland, M., Seyedin, M., Berven, S., and Lotz, J.C. Juvenile Chondrocytes May Facilitate Disc Repair. Open Tissue Eng Regen Med J **3,** 28, 2010.
56. Gorensek, M., Jaksimovic, C., Kregar-Velikonja, N., Gorensek, M., Knezevic, M., Jeras, M., Pavlovcic, V., and Cor, A. Nucleus pulposus repair with cultured autologous elastic cartilage derived chondrocytes. Cell Mol Biol Lett **9,** 363, 2004.
57. Sive, J.I., Baird, P., Jeziorsk, M., Watkins, A., Hoyland, J.A., and Freemont, A.J. Expression of chondrocyte markers by cells of normal and degenerate intervertebral discs. Mol Pathol **55,** 91, 2002.
58. Humzah, M.D., and Soames, R.W. Human intervertebral disc: structure and function. Anat Rec **220,** 337, 1988.
59. Roberts, S., Menage, J., Duance, V., Wotton, S., and Ayad, S. Collagen types around the cells of the intervertebral disc and cartilage end plate: an immunolocalization study. Spine **16,** 1030, 1991.
60. Cho, H.S., Park, S.H., Lee, S.M., Kang, M.J., Hasty, K.A., and Kim, S.J. Snapshot of degenerative aging of porcine intervertebral disc: a model to unravel the molecular mechanisms. Exp Mol Med **43,** 334, 2011.
61. Baer, A.E., Laursen, T.A., Guilak, F., and Setton, L.A. The micromechanical environment of intervertebral disc cells determined by a finite deformation, anisotropic, and biphasic finite element model. J Biomech Eng **125,** 1, 2003.
62. Pratsinis, H., and Kletsas, D. PDGF, bFGF and IGF-I stimulate the proliferation of intervertebral disc cells *in vitro* via the activation of the ERK and Akt signaling pathways. Eur Spine J **16,** 1858, 2007.
63. Chen, W.H., Lo, W.C., Lee, J.J., Su, C.H., Lin, C.T., Liu, H.Y., Lin, T.W., Lin, W.C., Huang, T.Y., and Deng, W.P. Tissue-engineered intervertebral disc and chondrogenesis using human nucleus pulposus regulated through TGF-beta1 in platelet-rich plasma. J Cell Physiol **209,** 744, 2006.
64. Gruber, H.E., Fisher, E.C., Jr., Desai, B., Stasky, A.A., Hoelscher, G., and Hanley, E.N., Jr. Human intervertebral disc cells from the annulus: three-dimensional culture in agarose or alginate and responsiveness to TGF-beta1. Exp Cell Res **235,** 13, 1997.
65. Alini, M., Li, W., Markovic, P., Aebi, M., Spiro, R.C., and Roughley, P.J. The potential and limitations of a cell-seeded collagen/hyaluronan scaffold to engineer an intervertebral disc-like matrix. Spine **28,** 446, 2003.
66. Thompson, J.P., Oegema, T.R., Jr., and Bradford, D.S. Stimulation of mature canine intervertebral disc by growth factors. Spine **16,** 253, 1991.
67. Kluba, T., Niemeyer, T., Gaissmaier, C., and Grunder, T. Human anulus fibrosis and nucleus pulposus cells of the intervertebral disc: effect of degeneration and culture system on cell phenotype. Spine **30,** 2743, 2005.
68. Park, S.H., Park, S.R., and Min, B.H. Reinforcement fibrin-hyaluronic acid composite gel for tissue engineering cartilage genesis. Key Eng Mater **342,** 253, 2007.
69. Yamaoka, H., Asato, H., Ogasawara, T., Nishizawa, S., Takahashi, T., Nakatsuka, T., Koshima, I., Nakamura, K., Kawaguchi, H., Chung, U.I., Takato, T., and Hoshi, K. Cartilage tissue engineering using human auricular chondrocytes embedded in different hydrogel materials. J Biomed Mater Res A **78,** 1, 2006.
70. Boudreau, N.J., and Jones, P.L. Extracellular matrix and integrin signalling: the shape of things to come. Biochem J **339,** 481, 1999.
71. Drury, J.L., and Mooney, D.J. Hydrogels for tissue engineering: scaffold design variables and applications. Biomaterials **24,** 4337, 2003.
72. Meinhart, J., Fussenegger, M., and Hobling, W. Stabilization of fibrin-chondrocyte constructs for cartilage reconstruction. Ann Plast Surg **42,** 673, 1999.
73. Chou, C.H., Cheng, W.T., Kuo, T.F., Sun, J.S., Lin, F.H., and Tsai, J.C. Fibrin glue mixed with gelatin/hyaluronic acid/chondroitin-6-sulfate tri-copolymer for articular cartilage tissue engineering: the results of real-time polymerase chain reaction. J Biomed Mater Res A **82,** 757, 2007.
74. Watson, D., Sage, A., Chang, A.A., Schumacher, B.L., and Sah, R.L. Growth of human septal chondrocytes in fibrin scaffolds. Am J Rhinol **24,** e19, 2010.
75. Eyrich, D., Brandl, F., Appel, B., Wiese, H., Maier, G., Wenzel, M., Staudenmaier, R., Goepferich, A., and Blunk, T. Long-term stable fibrin gels for cartilage engineering. Biomaterials **28,** 55, 2007.

Address correspondence to:
David L. Kaplan, Ph.D.
Department of Biomedical Engineering
Tufts University
4 Colby St.
Medford, MA 02155

E-mail: david.kaplan@tufts.edu

Received: April 4, 2011
Accepted: September 15, 2011
Online Publication Date: October 24, 2011